Structural Investigation of Pd(II) in Concentrated Nitric and Perchloric Acid Solutions by XAFS

J. Purans,*,†,‡,⊥ B. Fourest,† C. Cannes,† V. Sladkov,§ F. David,† L. Venault,|| and M. Lecomte||

Institut de Physique Nucléaire, 91406 Orsay CEDEX, France, Dipartimento di Fisica, Università di Trento, 38050 Povo (Trento), Italia, UBO-UFR Sciences et Techniques, 6 Av. Le Gorgeu, BP 809, 29285 Brest CEDEX, France, and CE VALRHO 30207 Bagnols sur Cèze, France

Received: October 4, 2004; In Final Form: March 29, 2005

XAFS spectra of palladium(II) in concentrated $HNO_3/HClO_4$ acid mixtures have been recorded and analyzed. Structural parameters of the $Pd(H_2O)_4^{2+}$ complex and the mixed nitric $Pd(NO_3)_2(H_2O)_2$ complex, for the first time, were determined by the XAFS method. For pure 5 M $HClO_4$ and for mixtures (0−0.3 M HNO_3), the XAFS spectra of the 0.02 M Pd solutions are indeed very similar and originated from four Pd−O_w equivalent distances. For the $Pd(H_2O)_4^{2+}$ square-planar aqua ion in strong perchloric acid, the use of an FEFF6 theoretical approach led to a first-shell Pd−O_w distance of 2.00 (1) Å and a Debye−Waller (DW) factor of $\sigma^2 = 0.0030$ (3) Å^2. Four water molecules are tightly bound to the Pd^{2+} ion in the equatorial plane, while two (or one) axial water molecules are weakly bound to the metal ion at 2.5 Å with a DW factor of 0.015 (5) Å^2. For highly concentrated mixtures (4−6 M HNO_3) and for pure concentrated (4−6 M) nitric acid as well as for crystalline powder $Pd(NO_3)_2(H_2O)_2$, the XAFS spectra are very similar and are determined by the mixed nitric complex $Pd(NO_3)_2(H_2O)_2$: four Pd−O near-equivalent distances of 2.01 (1) Å from two H_2O and two NO_3 molecules with a total DW factor of $\sigma^2 = 0.0037$ (3) Å^2. Moreover, two Pd---N distances of 2.8−2.9 Å were determined in the second coordination shell. Finally, for intermediate mixtures (1−3 M HNO_3 in 5 M $HClO_4$), the XAFS spectra are a superposition of the XAFS of $Pd(H_2O)_4^{2+}$ and $Pd(NO_3)_2(H_2O)_2$ complexes. The mean ligand number NO_3^- around Pd^{2+} has been calculated, and the XAFS results at pH close to zero confirm the spectrophotometric results previously published.

Introduction

Many long-lived fission products formed in nuclear spent fuels are elements of interest for the long-term radiotoxicity of high-level wastes. The impact of their storage on the environment is a problem of great importance; in solving this problem, a strategy coupling separation processes, transmutation, and specific conditioning is to be considered. Palladium-107 is one of these long-lived fission products, and its behavior in aqueous solutions needs, consequently, to be well-known. In particular, the nature of the aqueous ions in nitric media is still controversial.

The pioneering works of the Elding,[1] Jørgensen,[2] and Merbach[3] groups have made substantial contributions toward an understanding of the structure and mechanisms of substitution processes at four-coordinated square-planar Pd(II) complexes. This geometrical arrangement is highly favorable for the d^8 Pd(II) as well as for the Pt(II) electronic configuration due to the ligand field effect. It is also compatible with experimental data reported for different Pd(II) complexes, both in the solid phase and in solution, using many solvents (DMSO, CH_3CN, and H_2O), ligands (Cl^-, NO_3^-, ...), and counterions.[4,5]

Nowadays it is well established that a thorough understanding of many chemical properties of ionic solutions should be based on a precise knowledge of their coordination geometry. However, structural data for the ground-state species (for example $Pd(H_2O)_4^{2+}$ and $Pd(H_2O)_2(NO_3)_2$) are quite limited. Moreover, synthesis and characterization of solid-state crystalline Pd(II) hydrates have not been reported so far. This might be due to the low yield in their synthesis, which is probably related to the stability of the complex. A highly acid mixture of $HClO_4/HNO_3$ is necessary to avoid precipitation risk and to limit hydrolysis in order to characterize equilibrium between pure $Pd(H_2O)_4^{2+}$ aqua ions and mixed $Pd(NO_3)(H_2O)_3^+$, $Pd(NO_3)_2(H_2O)_2$, and $Pd(NO_3)_3(H_2O)^-$ nitrate complexes.[1−3]

Only $[Pt(H_2O)_4]^{2+}$, which can be taken as an analogue of $[Pd(H_2O)_4]^{2+}$, has been characterized by XAFS (X-ray absorption fine structure) technique.[5,6] Note that the LAXS (large-angle X-ray scattering) technique requires too high concentrations and long exposure times to be applicable to the solutions of the hydrated cations available.[5] Information on the Pd−O bonding distance as well as the possible presence of axially coordinated, weakly bound solvent molecules is still lacking. Nevertheless, a theoretical modeling of water exchange on both $Pd(H_2O)_4^{2+}$ and $Pt(H_2O)_4^{2+}$ has led to the definition of similar optimized structures for both tetraaqua ions with M−O distances (2.04 Å) within 0.03 Å of the experimental result for $Pt(H_2O)_4^{2+}$.[7] For Pd(II), the calculated M−O distance is thus 2.01 Å.[7]

The availability of the crystalline $Pd(NO_3)_2(H_2O)_2$ as a reference compound is especially valuable for the accurate structural characterization of Pd(II) in mixed perchloric and

* Author to whom correspondence should be addressed at Dipartimento di Fisica, Università di Trento, Via Sommarive, 14, I-38050 Povo (Trento), Italy. Phone: +39-0461-88 16 79. Fax: 39-0461-88 16 96. E-mail: purans@science.unitn.it.

† Institut de Physique Nucléaire.

‡ Università di Trento.

§ UBO-UFR Sciences et Techniques.

|| CE VALRHO.

⊥ Permanent address: Institut of Solid State Physics, University of Latvia, LV-1603 Riga, Latvia. E-mail: xas@latnet.lv.

10.1021/jp045489n CCC: $30.25
Published on Web 04/30/2005

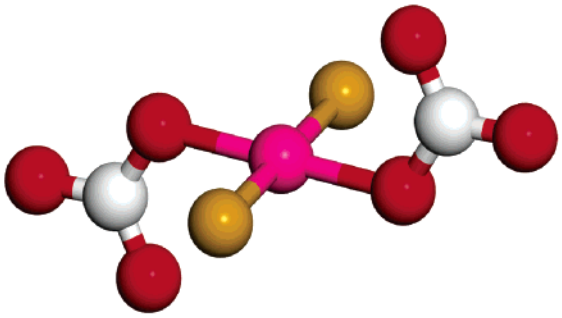

Figure 1. Schematic structure of $Pd(NO_3)_2(H_2O)_2$ molecule in crystalline $Pd(NO_3)_2(H_2O)_2$: Pd in the center; brown, O_w (H_2O, hydrogen atoms missing); red, O_N (NO_3^-); white, N (NO_3^-).

nitric acid solutions. The structure of orthorhombic $Pd(NO_3)_2(H_2O)_2$ (see Figure 1) was previously determined by X-ray powder diffraction and refined by the Rietveld method with medium accuracy.[8]

The first aim of the present work was to determine by XAFS the structure of Pd(II) in both perchloric and nitric acids. The experimental K-edge XAFS spectra of Pd^{2+} in aqueous solutions were analyzed using the multiple-scattering formalism. The second objective was to have a better knowledge of the complexation of Pd(II) by nitrate ions, by varying the nitrate concentration in a large range. As a matter of fact, the published stability constants concerning the system Pd(II)/NO_3^- are very scattered.[2,9−14]

In the final stage of this paper submission, a new theoretical paper[15] on the molecular dynamics study of the solvation phenomenon for a square-planar hydrate, $[Pd(H_2O)_4]^{2+}$, appeared. The first peak at the calculated RDF, centered at 2.00 Å, corresponds to the first-shell water molecules and integrates to four water molecules, while the second peak appearing at 2.67 Å integrates to two water molecules.

Experimental Section

It is generally accepted that perchlorate forms only very weak complexes with most ions,[16] and it is considered that significant complex formation between the soft Pd^{2+} and the hard perchorate anion is especially unlikely.[17,18] A highly acid mixture of $HClO_4/HNO_3$ was necessary to avoid precipitation risk and to limit hydrolysis in order to characterize equilibrium between pure $Pd(H_2O)_4^{2+}$ aqua ions and mixed $Pd(NO_3)(H_2O)_3^+$, $Pd(NO_3)_2(H_2O)_2$, and $Pd(NO_3)_3(H_2O)^-$ nitrate complexes.[1−3,8,18] Therefore, concentrated perchloric and nitric acids were used as the noncomplexing and the most complexing medium, respectively.

Preparation of the Samples. *Mother Solution.* A 0.12 M palladium stock solution in 5 M $HClO_4$ was prepared as described elsewhere.[19] Briefly, $Pd(OH)_2$ precipitate was prepared by adding an excess of NaOH (6 and 1 M) to a $HClO_4$ (1 M) solution containing 0.05 M $Pd(NO_3)_2$. The hydroxide was then washed four times with deionized water and dissolved in 5 M $HClO_4$. The palladium mother solution was centrifuged (5 min at 3500 rpm) and filtered at 0.2 μm. The concentration of the final solution was determined by spectrophotometry and confirmed by the measurements of the X-ray absorption jump at the Pd K-edge (see below).

XAFS Samples. The liquid samples were prepared by diluting 1.25 mL of 0.12 M Pd(II) mother solution in an appropriate volume of nitric acid (see Table 1) and a complementary volume of 5 M perchloric acid in order to obtain a total volume of 5 mL. The palladium concentration was then 0.02 M in the XAFS samples: this was chosen to be high enough to give an XAFS signal with high accuracy and sufficiently low to avoid precipitation at the pH studied. Prior to the measurements, the palladium solutions were centrifuged (5 min at 3500 rpm) in order to eliminate the colloids which could be formed.

TABLE 1: Amount of Nitric Acid and Perchloric Acid (5 M) Added for the Preparation of XAFS Samples; Resulting HNO_3 Concentration and $HClO_4$ Concentration

sample	V_{HNO_3}	V_{HClO_4}	$[HNO_3]$ (M)	$[HClO_4]$ (M)
SN1		3.75 mL	0	3.75
SN2	3 mL (0.5 M)	0.75 mL	0.3	0.75
SN3	0.5 mL (5 M)	3.25 mL	0.5	3.25
SN4	1 mL (5 M)	2.75 mL	1	2.75
SN5	3 mL (5 M)	0.75 mL	3	0.75
SN6	1.35 mL (15 M)	2.4 mL	4	2.4
SN7	1.7 mL (15 M)	2.05 mL	5	2.05
SN8	2 mL (15 M)	1.75 mL	6	1.75

An X-ray absorption cell with Kapton windows was used for the XAFS transmission measurements of solutions. The optical length was optimized to give a good absorption jump and to minimize the absorption of the bulk solution. The measurements were done at an optical length of 40 mm, resulting in values of the absorption jump of about 0.5 for Pd K-edge that corresponds to about 0.02 M, the concentration expected in the solutions. Therefore, XAFS spectra with high accuracy were measured. Moreover, the kinetics of Pd(II) precipitation was followed by successive scans after 1 h, 4 h, 10 h, and so forth, in the XANES region, and the change of the absorption jump was controlled.

The reference crystalline compounds $Pd(NO_3)_2(H_2O)_2$ (99.9%, ~40% of Pd, STREM chemicals) and PdO (STREM chemicals) were finely ground and mechanically mixed with cellulose powder to give pressed pellets with thickness chosen to obtain an absorption jump value of about 0.5 for Pd K-edge. The light-brown powder $Pd(NO_3)_2(H_2O)_2$ is more-or-less stable in air and decomposes into PdO.[8] However, an XAFS measurement is very sensitive to the formation of PdO, and therefore the samples were checked. The XAFS spectra have shown that no PdO was formed in the samples under study.

XAFS Measurements. XAFS measurements were performed at the LURE synchrotron radiation facility (Orsay, France) on the DCI D44 (XAS 4) beam line. Positron-beam energy and average current were 1.85 GeV and 320−250 mA, respectively. The XAFS spectra at the Pd K-edge (24350 eV; 24200−25050 eV) were measured in transmission mode. The synchrotron radiation was monochromatized by the Ge(400) double-crystal monochromator. The experimental spectra were measured using two ionization chambers (the first filled with Ar and the second filled with Kr) with a count rate of 2 s per point, an energy resolution of 7 eV. The calibration of the spectrometer was carried out using a thick palladium foil. At least 10 complete and identical XAFS scans were collected for each sample. Each spectrum was checked individually before averaging. All samples were measured at room temperature.

XAFS Data Analysis. The experimental XANES (Figure 2) and XAFS signals (Figure 3) at the Pd K-edge were treated using the EDA software package[20] in a way similar to the one used in the study of the Eu^{2+} and Sr^{2+} aqua ions.[21] The obtained XAFS spectra, $\chi(E)$, were converted to the k-space of the photoelectron wavevector, defined as

$$k = \sqrt{(2m/\hbar^2)(E - E_0)}$$

where $(E - E_0)$ is the photoelectron kinetic energy measured.

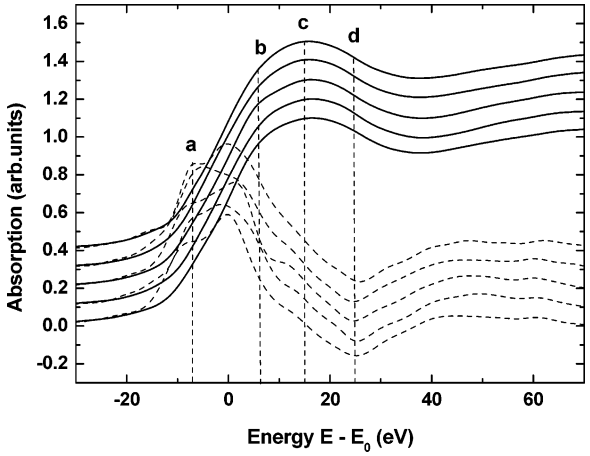

Figure 2. Variation of the normalized absorption coefficients in the XANES region (full lines) and their first derivatives (doted lines) at the Pd K-edge. Experimental XANES spectra of 0.02 M palladium(II) in concentrated $HNO_3/HClO_4$ acid mixtures (see Table 1) in comparison with the reference spectrum ($Pd(NO_3)_2(H_2O)_2$) are plotted on the same vertical scale and displaced vertically for clarity (from bottom to top): $Pd(NO_3)_2(H_2O)_2$ crystal; SN1 (0.0 M HNO_3); SN3 (0.5 M HNO_3); SN6 (4.0 M HNO_3); SN8 (6.0 M HNO_3). The energy scale is relative to the E_0-position. The E_0-position, defining the zero photoelectron wavevector value ($k = 0$), was set at the maximum of the first derivatives found by the alignment of the experimental XAFS signals. Main features are labeled by letters from **a** to **d**.

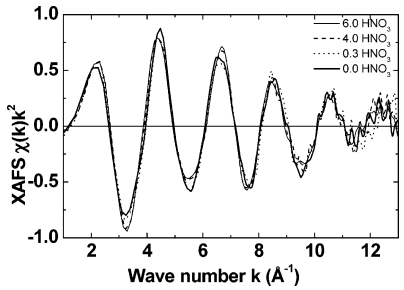

Figure 3. Experimental XAFS spectra of 0.02 M palladium(II) in concentrated $HNO_3/HClO_4$ acid mixtures (see Table 1): SN1 (0.0 M HNO_3), solid thick line; SN2 (0.3 M HNO_3), dotted line; SN6 (4.0 M HNO_3), dashed line; SN8 (6.0 M HNO_3), solid thin line.

The energy E_0 was located at the maximum of the first derivatives (see Figure 2). The experimental XAFS spectra $\chi(k)$ given in Figure 3 are multiplied by a factor k^2 to compensate for the decrease of amplitude with increasing wavevector value. The experimental XAFS spectra (Figure 3) were Fourier transformed (FT) with a Kaiser−Bessel window in the 0−13 $Å^{-1}$ range using a photoelectron phase shift and amplitude (Pd−O) corrections. The use of the phase-shift correction allowed us to reduce the nonstructural peaks distorting the baseline and led to a significant sharpening of the FT peaks, allowing a more precise Fourier filtering and interpretation of data.

Due to the lack of an appropriate solid reference compound that mimics the possible environment of the Pd^{2+} ion in aqueous solutions, it is extremely important to determine the theoretical phase and amplitude with the highest absolute accuracy. The theoretical phases $\phi(\pi,k)$ and amplitudes $\times a6(\pi,k)$ were calculated by FEFF6 code:[23] ab-initio quantum-chemical calculation by using self-consisted potential with complex Hedin−Lundqvist exchange-correlation part. The choice of different clusters that mimic the possible environment of the Pd^{2+} ion in the solutions will be discussed later in the article.

Multielectron Transition Effect. A number of authors has already discussed (see, for example, refs 21, 22) the presence of anomalous features in the Sr^{2+} and Ln^{3+} aqua ion XAFS spectra. In most cases, the multielectron transitions (MET) do not disturb the XAFS analysis, as their intensities are low compared to the oscillation amplitude. In the case of Pd(II), these anomalies result after FT in humps distorting the base of the major peak standing for the first-sphere Pd−O peak, especially at low distances at 1 Å (see Figure S1 presented in the Supporting Information). These humps prevent good first-shell filtering of the experimental XAFS spectra by back Fourier transform. Therefore, only structural information in the interval from 1.5 to 4.5 Å are presented and discussed in the next FTs.

Results and Discussion

Jørgensen and Parthasarathy[2] have demonstrated that, in concentrated perchloric acid, Pd(II) aqua ion is the unique species up to 0.01 M total palladium. It is generally accepted that perchlorate forms only very weak complexes with most ions.[16,17] On the other hand, in nitric aqueous solution, at pH close to zero, Pd(II) forms a mono-nitrato complex with $\beta_1 = (1.2 \pm 0.4)$.[2] Therefore, concentrated perchloric and nitric acids were used in this work as the noncomplexing and the most complexing medium.

XANES Experimental Data. The XANES structure for the solutions studied ($HNO_3/HClO_4$ acid mixtures) and for the crystalline $Pd(NO_3)_2(H_2O)_2$ sample are very similar and rather featureless (see Figure 2). Note that the low resolution at the Pd K-edge, which is due to the large natural broadening and experimental resolution equal to 7 eV, results in a smearing of the details in the XANES region. Nevertheless, the singularities presented well at the first derivatives of the XANES spectra (see Figure 2). Note that the energy scale is relative to the E_0-position. The E_0-position, defining the zero photoelectron wavevector value ($k = 0$), was set at the maximum of the first derivative of the experimental XAFS signals. Main features are labeled by letters from **a** to **d**.

A preedge shoulder at about −7 eV (indicated by **a** in Figure 2), the inflection points at about 6 eV and at about 25 eV (indicated by **b** and **d**, respectively), and the maximum at about 15 eV (indicated by **c**), as well as the singularities at their first derivatives of the solutions, are very similar to that of crystalline $Pd(NO_3)_2(H_2O)_2$. The spectra of the solutions and the crystalline $Pd(NO_3)_2(H_2O)_2$ sample superimpose, thus confirming that the PdO_4 square-planar coordination polyhedra are the same.

A typical characteristic of the Pd K-edge region, as for other 4d transition-metal oxides, is the presence of a preedge shoulder (indicated by **a** in Figure 2), located below the continuum threshold E_0. It originates from the 1s(Pd) → 4d(Pd) + 2p(O) transition, in which the final state of the electron is the relaxed excited state in the continuum with 4d(Pd) atomic character in the presence of the core hole at the 1s(Pd) level screened by other electrons. For example, such a transition is forbidden in the dipole approximation for a perfect octahedron, the preedge shoulder amplitude depends on the degree of the PdO_6 octahedron distortion and on that of the 2p(O)-4d(Pd) hybridization. The PdO_4 configuration is strongly favorable for the 1s(Pd) → 4d(Pd) + 2p(O) transition, which explains the origin of the preedge shoulder. The nearest group of oxygen atoms gives the main contribution to the shoulder in the spectra.

However, the interpretation of X-ray absorption near-edge structure at the Pd K-edge in the solutions has to be done in the future within full multiple scattering formalism to answer this point. The preliminary XANES calculation within the full multiple scattering formalism on the cluster of $Pd(NO_3)_2(H_2O)_2$

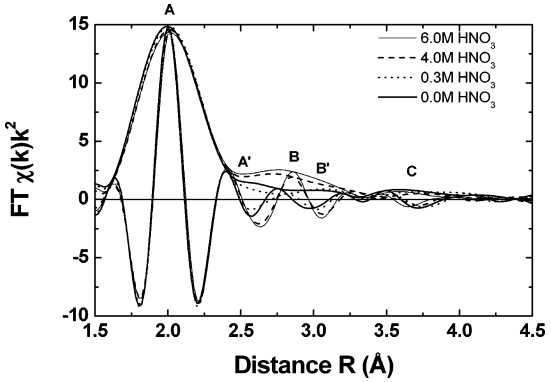

Figure 4. Part of Fourier transforms (modulus and imaginary parts) of experimental XAFS spectra of 0.02 M palladium(II) in concentrated $HNO_3/HClO_4$ acid mixtures: SN1 (0.0 M HNO_3), solid thick line; SN2 (0.3 M HNO_3), dotted line; SN6 (4.0 M HNO_3), dashed line; SN8 (6.0 M HNO_3), solid thin line. These Fourier transforms have been corrected for the photoelectron phase shift using the theoretical phase and amplitude (see text for details).

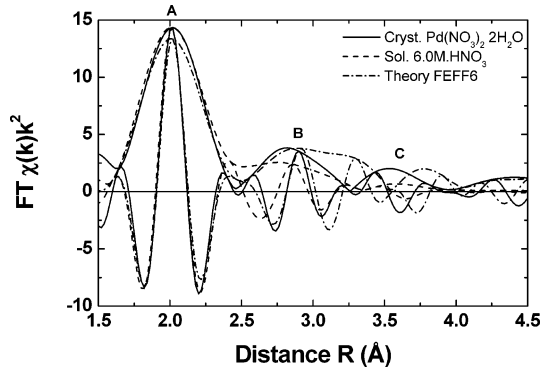

Figure 5. Fourier transforms (modulus and imaginary parts) of the experimental XAFS spectra of $Pd(NO_3)_2(H_2O)_2$ powder (solid line) and 0.02 M Pd(II) in 6 M HNO_3 solution (dashed line) in comparison with the theoretical MS FEFF6 calculation for $Pd(NO_3)_2(H_2O)_2$ crystal (dashed doted line). These Fourier transforms have been corrected for the photoelectron phase shift using the theoretical phase and amplitude (see text for details).

is shown in the Supporting Information (Figure S2). Further details will be presented elsewhere (Purans et al., to be published).

XAFS Experimental Data. The XAFS spectra are presented in Figure 3. The XAFS signals features are very similar among the high-concentration solutions of HNO_3 (4−6 M). On the other hand, the XAFS signals features are very similar among the low-concentration solutions of HNO_3 (less than 1 M) and pure 5 M perchlorate solution, while an intermediate XAFS spectrum is observed for the solutions with intermediate concentrations, HNO_3 varying from 1 to 3 M. Consequently, the first and second types of the FT are presented in Figure 4. Finally, the FTs obtained under similar conditions for the crystalline $Pd(NO_3)_2(H_2O)_2$ and the solution of Pd(II) in 6 M HNO_3 are compared in Figure 5.

The FTs given present a series of peaks corresponding to single-scattering (SS) and multiple-scattering (MS) contributions of oxygen and nitrogen atoms around the Pd ion. Each FT presented in Figures 4 and 5 has a first dominant peak well superimposed at 1.6−2.5 Å with a maximum at 2.0 Å (label A), corresponding to the first coordination shell of Pd−O. Moreover, for high HNO_3 concentrations (3−6 M) and for crystalline $Pd(NO_3)_2(H_2O)_2$ (see Figure 5), a second peak located at 2.5−3.2 Å with a maximum at 2.8 Å (label B) and a third peak at 3.4−4.0 Å with a maximum at 3.7 Å (label C) are clearly visible. While for a low nitrate concentration less than 1 M, as well as in pure perchlorate solution, small peaks are observed around 3.0 Å (label B′) and around 3.7 Å (label C). Moreover, a hump appears at about 2.5 Å (label A′). We conclude that, with respect to the pure perchloric acid solution, the presence of nitrate in the mixed solutions greatly increases the second-shell peak (label B), whereas nitrate has a much lesser influence on the first-shell peak (label A).

The availability of the crystalline $Pd(NO_3)_2(H_2O)_2$ as a reference compound is especially valuable for the accurate structural characterization of nitric acid solutions. The FT functions obtained under similar conditions for the crystalline $Pd(NO_3)_2(H_2O)_2$ and the solution of Pd(II) in 6 M HNO_3 show interesting similarities in Figure 5. The XAFS observed for the solution of Pd(II) in 6 M HNO_3 and the crystalline $Pd(NO_3)_2(H_2O)_2$ indicate that the coordination around palladium is very similar in the solution and in the crystal, despite the difference in the amplitude of B and C peaks due to a structural disorder in solutions. The first peak assigned to the Pd−O bonds presents the same maximum at a distance of 2.01 (1) Å, which is very close to the mean distances Pd−O_w (from H_2O molecule) and Pd−O_N (from nitrate group) found by Caminiti et al.:[24,25] 2.02 Å and 2.0 Å, respectively. The second peak due to the Pd---N single scattering contribution is, as expected by calculations (see below), much wider and flatter in the case of the solutions (structural disorder), compared to the crystal, and the distance Pd---N is a little shorter in the solution (2.85 Å) in comparison with the crystal (2.90 Å). Therefore, the second-shell interatomic distance obtained in the crystal is in good agreement with that proposed by Laligant et al.:[8] 2.846 Å.

XAFS Analysis of Pd(II) Aqua Ion in Pure Perchlorate Solution. The theoretical phases $\phi(\pi,k)$ and amplitudes $\phi(\pi,k)$ were calculated by FEFF6 code for a regular PdO_4 square-planar cluster using a muffin-tin (MT) approximation with MT radii of 0.74 Å for oxygen and 1.14 Å for palladium, as in the case of reference $Pd(NO_3)_2(H_2O)_2$ compound (see below).

The single-shell XAFS spectra were fitted using the single-scattering curved-wave formalism in a way similar to the one used in ref 21. The SS contributions, related to the first shell, were singled out by the back FT with phase and amplitude corrections in the interval 1.5−2.5 Å. The best fit of the XAFS signals analysis was performed in the k range from 1.5 to 12.5 $Å^{-1}$. For the $Pd(H_2O)_4^{2+}$ square-planar aqua ion in a strong perchloric acid, the use of an FEFF6 theoretical approach[23] led to a first-shell Pd−O_w distance of 2.00 (1) Å with four water molecules and a very small Debye−Waller (DW) factor of $\sigma^2 = 0.0030$ (3) $Å^2$. The fitting procedure was also performed for unfiltered spectra, and the structural parameters determined were equal (within error bar of experiments) to ones obtained for the individual filtered first shell.

The refined fitting parameters are in close agreement with those for the $Pt(H_2O)_4^{2+}$ square-planar aqua ion previously reported by Hellquist et al.[5] (2.01 Å) and Ayala et al. (2.02 Å).[6] Moreover, the structure of $Pd(H_2O)_4^{2+}$ is also in close agreement with the theoretical parameters of $Pd(H_2O)_4^{2+}$ aqua ion reported by Deeth and Elding[7] (2.01 Å) and recently reported by the Marcos group (2.00 Å).[15]

Another feature to consider is the possible role of solvent molecules loosely coordinated along the z-axis of the planar complexes. To understand the origin of the peaks in the FT spectra beyond the first shell, we have additionally included in the FEFF6 calculation one or two axial water molecules and eight hydrogen atoms of four water molecules in the plane. Unfortunately, there is a difficulty in regard to the inclusions

of hydrogen atoms in the FEFF code.[6,21,26,27] This difficulty exists because the O−H bond is much shorter than the Pd−O distance, and for the oxygen and hydrogen it is difficult to determine a good muffin-tin radius: FEFF code gives unrealistic muffin-tin radii and an overestimation of the backscattering contribution.[21,26,27]

Here, to resolve this problem, we have used a known approximation by substituting the backscatter with the next chemical element. Thus, hydrogen atoms have been substituted by helium atoms in the FEFF calculation. "Water molecules" following the Benfatto et al. paper[28] on Cu^{2+} have been placed for simplicity in the so-called "dipole" configuration, according to which the ion, oxygen, and two hydrogen atoms lie in one plane. Note, that SS and MS contributions in the chain Pd−O−H are not sensitive to the orientation of the hydrogen atoms. Phase shifts have been calculated using MT radii of 0.35 and 0.65 Å for helium and oxygen, respectively, and 1.25 Å for palladium. We have also repeated the Benfatto et al.[28] analysis on Cu(II) in order to establish the accuracy of this approximation. We have obtained the water molecules at a planar position copper−oxygen distance about 1.95 Å and at apical positions with a copper−oxygen distance about 2.4 Å, while the copper−hydrogen distance is about 2.7 Å, in good agreement with previously published results.[28]

We have tested three structural models of Pd^{2+}: (i) PdO_{4pl}, square-planar cluster; (ii) $PdO_{4pl}O_{2ax}$, square-planar cluster with two axial oxygens; and (iii) $PdO_{4pl}H_8O_{2ax}$, square-planar cluster with two axial oxygens and eight hydrogens. We have followed the Benfatto et al.[28] analysis by MSXAS and GNXAS codes of the XAFS data of Cu(II) solutions in order to establish the water molecules at apical positions with a metal−oxygen distance about 2.5−3.0 Å and a metal−hydrogen distance about 2.7 Å.

The first model was the regular PdO_{4pl} square-planar cluster with $Pd-O_{pl}$ of 2.00 Å (given by XAFS). The calculated SS and MS paths and related XAFS signals, which produce the largest contribution, are presented in Figure 6a. The two curves in Figure 6a are the $Pd-O_{pl}$ equatorial first-shell SS signals and the MS contribution associated with the two linear $O_{pl}-Pd-O_{pl}$ configurations of the equatorial plane. Note that thermal damping was included by multiplying the signals with one DW factor = 0.003 Å^2 (the value obtained for the first shell by XAFS). The FT is shown in Figure S3 (see Supporting Information). Feature A (2.00 Å) is due to the single-scattering by four oxygen atoms of the first shell. The $O_{pl}-Pd-O_{pl}$ signal is responsible for the origin of the third peak C at 3.7 Å. The calculated (first model) and experimental signals become similar except for the B′ peak at 2.8−3.0 Å and the shoulder A′ at 2.5 Å.

The second model was $PdO_{4pl}O_{2ax}$: the regular PdO_{pl} square-planar cluster with two long axial oxygens $Pd-O_{ax}$ at 2.5 Å with the angle $O_{pl}-Pd-O_{ax} = 90°$. This model was used to check the importance of the contribution from axial oxygens (SS signals) versus the SS and MS contributions from the regular PdO_{pl}. The thermal damping (DW factor) was included: one for PdO_{pl} square-planar oxygens (as in the first model) by multiplying the signals with one DW factor = 0.003 Å^2, and the second for PdO_{ax} axial oxygens (loosely bonded water molecule) by multiplying the signals with a large DW factor = 0.015 Å^2 taken as in the fitting results (see below). The calculated SS and MS paths and related XAFS signals, which produce the largest contribution, are presented in Figure 6a. The total XAFS signal for the $PdO_{pl}O_{ax}$ cluster is also shown in Figure 6a. The three last curves from the top are the $Pd-O_{pl}$ equatorial and $Pd-O_{ax}$ axial first-shell SS signals, and the MS

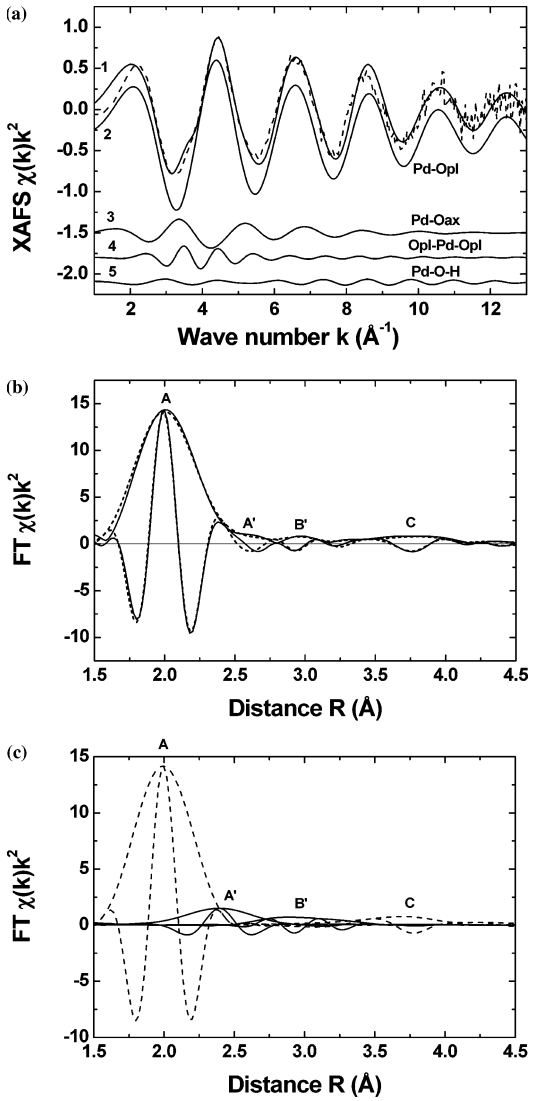

Figure 6. (a**)** Comparison between the theoretical MS XAFS spectrum of $PdO_{4pl}H_8O_{2ax}$ cluster (solid line) and the raw experimental data (dashed line) of 0.02 M palladium(II) in the concentrated $HClO_4$ solution: 1, total calculated MS XAFS spectra of $PdO_{4pl}H_8O_{2ax}$; 2, SS contribution from four planar oxygens $Pd-O_{4pl}$; 3, SS contributions from two axial oxygens of $Pd-O_{2ax}$; 4, MS contributions from four planar oxygens $Pd-O_{4pl}$; 5, SS and MS contributions from eight planar hydrogens Pd---H_8. Theoretical XAFS spectra are plotted on the same vertical scale and displaced vertically for clarity. **(b)** Fourier transforms (modulus and imaginary parts) of theoretical XAFS spectrum of the $PdO_{4pl}H_8O_{2ax}$ cluster (solid line) in comparison with the raw experimental data of $Pd(H_2O)_4^{2+}$ (dashed line). These FT have been corrected for the photoelectron phase shift using the theoretical phase and amplitude (see text for details). **(c)** Partial SS and MS contributions of the different atoms to the Fourier transform (modulus and imaginary parts) of theoretical XAFS spectra calculated for the $PdO_{4pl}H_8O_{2ax}$ cluster: dashed line (A peak), SS contribution of four planar oxygens ($Pd-O_{4pl}$); solid line (A′ peak), SS contribution of two axial oxygens ($Pd-O_{2ax}$); solid line (B′ peak), total contribution (SS and MS) of hydrogens ($Pd-O_{pl}-H$); dashed line (C peak), MS contributions of four planar oxygens $Pd-O_{4pl}$. These FT have been corrected for the photoelectron phase shift using the theoretical phase and amplitude (see text for details).

contributions associated with the two linear $O_{pl}-Pd-O_{pl}$ configurations of the equatorial plane. Note that MS signals associated with the rectangular configurations and the O−Pd−O axial path are negligible in this energy range. The FT is shown in Figure S3 (see Supporting Information). For the second model, the calculated and experimental FT signals become

TABLE 2: First-Shell Structural Parameters for the Aqueous 0.02 M Pd(II) Solution Obtained from the XAFS Data Analysis Assuming 4-fold, 5-fold, and 6-fold Coordination Models[a,b]

model	paths	N[c]	R^d (Å)	$\sigma^{2\,e}$ (Å^2)	$\epsilon^f \times 10^3$
6-fold coord.					
Pd−O_{pl}	SS	4	2.001 (5)	0.0032 (3)	
Pd−O_{ax}	SS	2	2.5 (1)	0.015 (5)	2.7
Pd---H_8	SS	8	2.9 (2)	0.015 (5)	
O_{pl}−Pd−O_{pl}	MS	4	3.9 (1)	0.025 (5)	
5-fold coord.					
Pd−O_{pl}	SS	4	1.999 (5)	0.0035 (3)	
Pd−O_{ax}	SS	1	2.5 (1)	0.009 (5)	2.2
Pd---H_8	SS	8	2.9 (2)	0.012 (5)	
O_{pl}−Pd−O_{pl}	MS	4	3.9 (1)	0.024 (5)	
4-fold coord.					
Pd−O_{pl}	SS	4	1.997 (5)	0.0034 (3)	
Pd−O_{ax}	SS	0			4.4
Pd---H_8	SS	8	2.7 (2)	0.005 (5)	
O_{pl}−Pd−O_{pl}	MS	4	3.9 (1)	0.028 (5)	

[a] The coordination number is fixed inside the model. [b] Estimated errors are presented within parentheses. Values in parentheses refer to a standard deviation. [c] N is the coordination number. [d] R is the metal−oxygen average distance. [e] σ^2 is the DW factor. [f] ϵ is the error function value (see ref 21).

similar also for shoulder A′ at 2.5 Å. So, the calculated and experimental signals become similar (A, A′, and C), except for the B′ peak at 2.8−3.0 Å.

The third model was $PdO_{4pl}H_8O_{2ax}$. The DW factors for the oxygens were included as in the second model, while for the hydrogens, the DW factor of 0.015 Å^2 was taken as in the fitting results (see below). The FTs are compared in Figure 6b, and the calculated and experimental signals become similar also for the B′ peak at 2.8−3.0 Å. Partial contributions of the SS and MS paths to the total FT are shown in Figure 6c.

Finally, three different coordination models have been used in the fitting procedure. In particular, the XAFS data have been fitted with hydrogen and without hydrogen contribution, assuming the presence of four water molecules in the equatorial plane and zero, one, or two axial oxygens. During the fitting procedure, the coordination numbers have been kept fixed. The structural parameters obtained from the fitting procedures are reported in Table 2, while the corresponding fitting parameters are reported in Table S1. The results obtained for the six-, five- and 4-fold-coordinated complexes are shown in the upper, middle, and lower panels of Table S1, respectively.

The result of this analysis is that the XAFS experimental data can be reproduced with the same accuracy, using both a 5-fold or a 6-fold coordination. In particular, the DW factors and the coordination numbers associated with the axial oxygens are highly correlated, and this hampers a unique determination of these parameters. On the other hand, the XAFS theoretical spectra associated with the fitted 5-fold and 6-fold models are in much better agreement with the experimental data, as compared to the 4-fold one. In particular, in the latter case the theoretical curve is not able to completely reproduce the hump appearing at about 2.5 Å (label A′) feature associated with the axial oxygens. This finding is confirmed by the increase of the error function value ϵ going from the square-planar model to the distorted octahedral model.

However, the interesting question remains: "What is the second hydration shell contribution in the EXAFS′?" The problem is usually explained by strong first-shell MS contributions competing with the second hydration shell signal.[27,29−31] Also, in the simplest case, as octahedral aqua ions (Cr^{3+} and Zn^{2+}), controversy exists. For example, in the recent paper of Campel et al. is reported that the second shell of Cr^{3+} is responsible only for about 1/3 of the XAFS FT signal at the position of the second shell.[31] Therefore, the interpretation of the second hydration shell at the Pd K-edge XAFS in the solutions has to be done in the future within full multiple scattering formalism and MD simulation to answer this point.

To conclude about MS analysis, the XAFS data strongly indicate that the hydrated Pd^{2+} ion binds four water molecules arranged in a square plane at 2.00 Å and with a DW factor of 0.003 Å^2, and that a further two (or one) weakly bound water molecules are bound at the apical sites at 2.5 Å with a great DW factor of $\sigma^2 = 0.015$ Å^2.

Lets Compare the Results Obtained with Previously Published Data. On one hand, Deeth and Elding[7] have claimed that noteworthy attempts to detect axially coordinated solvent molecules by NMR, large-angle X-ray scattering (LAXS), and XAFS have given negative results.[6,7] On the other hand, Caminiti et al.[24,25] have applied a "sharpening" analysis of the LAXS data of highly concentrated Pd(II) and Pt(II) solutions in order to establish the water molecules at apical positions with a metal−solvent distance about 2.8 Å. Moreover, calculated by Deeth and Elding,[7] metal−axial water distances fall in the range of 2.6−2.8 Å with binding energies of about 5 kJ/mol (local density approximation LDA) and about −20 kJ/mol (gradient-corrected GC). That is, the axial water is weakly bound at the LDA level, while the GC calculations suggest no axial binding.

As we have written before, in the final stage of the paper submission, a new theoretical paper[15] on the molecular dynamics study of the solvation phenomenon for a square-planar hydrate, $[Pd(H_2O)_4]^{2+}$, appeared. The first peak at the calculated RDF, centered at 2.00 Å, corresponds to the first-shell water molecules and integrates to four water molecules, while the second peak appearing at 2.67 Å integrates to two water molecules. It points out that this geometry suggests a dynamical picture in which the axial oxygens undergo a fast exchange, while the planar oxygens undergo a slow exchange, with the second-shell water molecules.

Thus, our experimental result on the structure of $Pd(H_2O)_4^{2+}$ is also in close agreement with the theoretical model of $Pd(H_2O)_4^{2+}$ aqua ion reported by the Marcos group in 2004.[15]

XAFS Analysis of Crystalline $Pd(NO_3)_2(H_2O)_2$. The MS calculations were performed by FFEF6 code using the crystallographic data of $Pd(NO_3)_2(H_2O)_2$.[8] Phase shifts have been calculated using the muffin-tin (MT) approximation with MT radii of 0.76 and 0.61 Å, for oxygen and nitrogen, respectively, and 1.17 Å for palladium. The choice of the clusters $Pd(NO_3)_2(O_w)_2$ (see Figure 1) was based on the orthorhombic $Pd(NO_3)_2(H_2O)_2$ crystalline coordinates.[8]

The structure of orthorhombic $Pd(NO_3)_2(H_2O)_2$ was previously determined by X-ray powder diffraction and refined by the Ritveld method with medium accuracy.[8] Consequently, three coordination shells can be separated on the radial distribution function (RDF) around the Pd(II) ions. The first coordination shell achieves the square-planar coordination distorted as a consequence of two types of bond lengths: Pd−O_w (from H_2O, 2.095 Å) and Pd−O_N (from NO_3, 1.963 Å). The second coordination shell contains the contributions from two monodentate nitrato complexes: two nitrogen atoms (Pd---N of 2.846 Å) and two oxygen atoms (Pd---O_4 of 2.931 Å). The third coordination shell is very purely defined and contains 12 oxygen and nitrogen atoms (3.2 to 4.1 Å) from the next coordination shell water molecules and NO_3^-, and also a contribution from

TABLE 3: XAFS Parameters of the First and Second Coordination Shells as a Function of the [HNO_3]/[$HClO_4$] Concentrations in Aqueous 0.02 M Pd(II) Solutions[a]

sample; [HNO_3]:[HClO]	N_1[b]S_0	R_1[c] (Å)	σ_1^2[d] (Å^2)	N_2[b]S_0	R_2[c] (Å)	σ_2^2[d] (Å^2)	ϵ[e] × 10^3
cryst. $Pd(NO_3)_2(H_2O)_2$	4.2 (3)	2.006 (5)	0.0030 (3)	2.4 (3)	2.91 (5)	0.004	20
XRD data[f]	4.0	2.029		2.0	2.846		
SN1; 0 M:3.75 M	4.3 (3)	2.006 (5)	0.0030 (3)				12
SN2; 0.3 M:0.75 M	4.3 (3)	2.000 (5)	0.0030 (3)	0.2 (3)	2.77 (9)	0.004[g]	14
SN3; 0.5 M:3.25 M	4.6 (3)	2.004 (5)	0.0032 (3)	0.8 (3)	2.82 (5)	0.004[g]	30
SN4; 1 M:2.75 M	4.7 (3)	2.005 (5)	0.0037 (3)	0.7 (3)	2.87 (5)	0.004[g]	19
SN5; 3 M:0.75 M	4.3 (3)	2.009 (5)	0.0030 (3)	1.1 (3)	2.87 (5)	0.004[g]	15
SN6; 4 M:2.4 M	4.3 (3)	2.007 (5)	0.0031 (3)	2.0 (3)	2.85 (5)	0.004[g]	7
SN7; 5 M:2.05 M	4.6 (3)	2.010 (5)	0.0034 (3)	2.3 (3)	2.85 (5)	0.004[g]	9
SN8; 6 M:1.75 M	4.6 (3)	2.009 (5)	0.0037 (3)	2.5 (3)	2.86 (5)	0.004[g]	6

[a] Estimated errors are presented within parentheses. Values in parentheses refer to a standard deviation. [b] N is the coordination number. [c] R is the metal−oxygen average distance. [d] σ^2 is the DW Factor. [e] ϵ is the error function value (see ref 21). [f] These data have been arithmetically averaged from two types of bond lengths: Pd−O_w (from H_2O, 2.095 Å) and Pd−O_N (from NO_3, 1.963 Å) reported in ref 8. [g] Fixed.

two oxygen atoms (Pd---O_3 of 4.02 Å) of the NO_3^- first coordination shell.

The theoretical analysis of the XAFS signals was performed within an ab-initio MS model with known crystallographic data for a cluster within the 6-Å radius, taking into account all SS and MS paths up to the third order. The comparison of MS and SS calculations for the clusters of different dimensions allowed us to assign different peaks on the experimental XAFS FT. So the cluster within a 4.0-Å radius around Pd mimics well the crystal structure of $Pd(NO_3)_2(H_2O)_2$ and possible environment of Pd(II) in nitric solutions. Therefore, the MS calculations were reduced to the radius of 4.0 Å.

With the first step, we tried to understand qualitatively the nature of the peaks A at 1.5−2.5 Å, B at 2.4−3.3 Å, and C at 3.3−4.0 Å, beyond the first coordination shell in the XAFS FTs and particularly about the MS contributions. The more important SS paths (4) and all MS (9) paths are for the cluster of 11 atoms $PdO_4N_2O_4$ (that mimic well the molecule $Pd(NO_3)_2(H_2O)_2$): two oxygen atoms from the water molecule at R = 2.095 Å, two oxygen atoms from the $(NO_3)^-$ ion at R = 1.963 Å, two nitrogen atoms from the $(NO_3)^-$ ion at R = 2.846 Å, two oxygen atoms from the $(NO_3)^-$ ion at R = 2.931 Å, and two oxygen atoms from the $(NO_3)^-$ ion at R =4.0268 Å that strongly overlap with the third coordination shell around Pd. The SS calculation (4 paths) gives surprisingly good agreement with the experiment (see Figure 5). The modulus and imaginary parts of these FTs coincide well too. The MS signals give only a small distortion of the form of the SS contributions. The modulus and imaginary parts of these FTs coincide well too. The MS signals produce some contribution in the XAFS region and to the FT peak C; however, it seems that the MS signals produce a small contribution in the experimental spectra. This result is mainly due to the interference effect between MS signals and, possibly, structural and/or thermal disorder.

To conclude about MS analysis, we suggest that also on the experimental FTs the main first peak (A) corresponds to SS processes on the four oxygen atoms, the second (B) corresponds mainly to SS from the second shell around a palladium ion formed by the two nitrogen atoms and two other oxygen atoms, and peak C corresponds to MS contributions within near-linear Pd−N−O_3 chains and the third coordination shell. Its amplitude is damped by the dispersion of the distances structural and thermal disorder.

For the $Pd(NO_3)_2(H_2O)_2$ complex in the crystal under investigation, one-shell (Pd−O_{av}) and two-shell (Pd−O_w, Pd−ON) contribution models were used. We took three fitting parameters for the one-shell model (N·S_0, R, DW), and four fitting structural parameters for the two-shell model (R_1, DW_1, R_2, DW_2 with $N_1 = N_2 = 2$). Surprisingly, the one-shell model gives a small fitting error with a reasonable DW factor and amplitude of XAFS spectra (N·S_0 = 4.6). In contrast, the two-shell model with crystallographic distances Pd−O of 2.095 Å and 1.963 Å gives an unreasonably great fitting error with unreasonable coordination numbers. Therefore, only the one-shell model fitting results for the first coordination shell is presented in Table 3.

XAFS Analysis of $Pd(NO_3)_n(H_2O)_m$ Complexes in Solution. The MS calculations were performed by FFEF6 code using the crystallographic data of $Pd(NO_3)_2(H_2O)_2$ (see before). The peak observed at 2.0 Å and well superimposed on each XAFS spectrum should correspond both to the Pd−O_w (H_2O) and Pd−O_N (NO_3) bonds. This is in good agreement with the fact that the corresponding two bond distances are very close in the $Pd(NO_3)_2(H_2O)_2$ crystal, as mentioned earlier. Moreover, the peak observed at 2.85 Å when the nitrate concentration exceeds 3 M should correspond to the Pd---N distance. This distance is also very close to the value obtained in the case of the $Pd(NO_3)_2(H_2O)_2$ solid compound. The fact that we can observe only a shoulder at nitrate concentrations as high as 1−3 M and a small peak for higher concentration values tends to confirm that the complexation of palladium(II) by nitrate ions is rather weak for these concentrations.

First Coordination Shell Fitting Results. The single-shell XAFS spectra were fitted using the single-scattering curved-wave formalism. The SS contributions, related to the first shell, were singled out by the back FT in the intervals 1.5−2.5 Å (ΔR = 1.0 Å). The best fit of the XAFS signals analysis was performed in the k range from 1.5 to 12.5 Å^{-1} (Δk = 11.0 Å^{-1}) with theoretical phases $\phi(\pi,k)$ and amplitudes ×a6(π,k) calculated by FEFF6 code.

For $Pd(NO_3)_n(H_2O)_m$ complexes in the solutions under investigation, the one-shell model gives a small fitting error with reasonable coordination numbers (N·S_0 = 4.6), distances, and DW factors. Therefore, for the first coordination shell, one-shell model fitting results are only presented in Table 3.

Second Coordination Shell Fitting Results and Speciation of Pd(II) in Nitrate-Containing Solutions. The raw XAFS spectra without Fourier filtering were fitted using two-shell SS formalism (first and second shells). The best-fit analysis was performed in the k range from 1.5 to 12.5 Å^{-1} (Δk = 11.0 Å^{-1}) with theoretical phases $\phi(\pi,k)$ and amplitudes ×a6(π,k) calculated by FEFF6 code (see above). The two-shell model gives a small fitting error with reasonable distances, DW factors, and coordination numbers. Therefore, the fitting results are presented in Table 3.

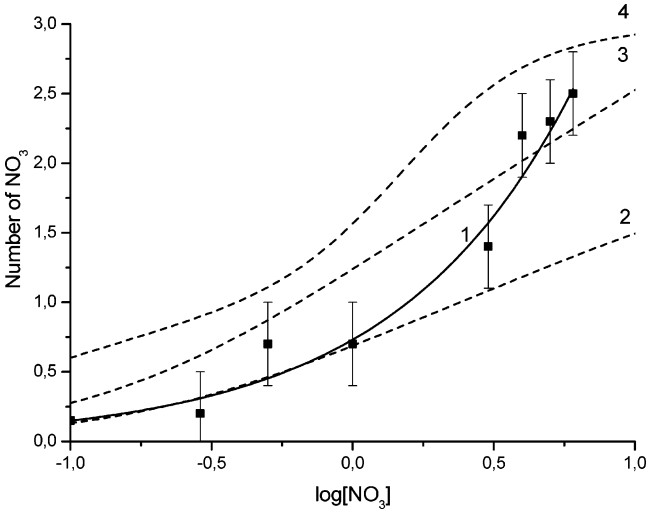

Figure 7. Mean number of nitrate ligand complexing Pd(II) calculated from the stability constants given in Table 3 in comparison with XAFS data: 1 (solid line), XAFS fitting results (this work); 2 (dashed line), Camacho et al.;[9] 3 (dashed line), Tarapcik;[10] 4 (dashed line), Shmidt.[11]

TABLE 4: Stability Constants Published in the Literature

source	β_1	β_2	β_3	β_4
Jørgensen et al.[a]	1.2 ± 0.4			
Camacho et al.[b]	1.47 ± 0.08	0.173 ± 0.015		
Shmidt et al.[c]	14	2	6	
Tarapcik[d]	3.28	2.13	0.223	0.004

[a] Ref 2. [b] Ref 9. [c] Ref 11. [d] Ref 10.

From the second shell (Pd---NO_3) coordination numbers collected in Table 3, the distribution of the $Pd(NO_3)_n(H_2O)_m$ species formed in nitrate media can be calculated and a mean ligand number, *n*, can be derived. These XAFS results are reported both in Table 3 and Figure 7.

The existence, in aqueous solutions, of two bound water molecules at the apical sites of $PtCl_4^{2-}$ and $PdCl_4^{2-}$ ions is pointed out by Caminiti et al.[24,25] using experimental LAXS technique (hump at 2.77 Å). They also suggested that in the case of concentrated 0.95−2.58 M nitrate solutions, Pd(II) is coordinated by two nitrates and two water molecules in the first shell, each of these first-shell water molecules being surrounded by three second-shell water molecules. The mean distances Pd−O_w (from H_2O molecule) and Pd−O_N (from nitrate group) are found to be close: 2.02 Å and 2.0 Å, respectively, and cannot be strictly compared to those determined ab initio from X-ray powder diffraction data on the solid $Pd(NO_3)_2(H_2O)_2$ compound,[8] 2.095 Å and 1.963 Å, respectively, despite the same square-planar geometry. Note that the apical sites of PdO_4 are vacant in the crystalline $Pd(NO_3)_2(H_2O)_2$.

Speciation of Pd(II) in Nitrate-Containing Solution. Jørgensen and Parthasarathy[2] have demonstrated that in nitric aqueous solution, at pH close to zero, palladium(II) forms a mono-nitrato complex with $\beta_1 = (1.2 \pm 0.4)$ L mol.$^{-1}$. The value of $\beta_1 = (1.47 \pm 0.08)$ L mol.$^{-1}$ obtained recently by Camacho et al.[9] is not significantly different from the value given by Jørgensen et al.[2] Nevertheless, at higher concentration of [NO_3^-], the papers[9−14] dealing with the complexation of Pd(II) by nitrate ligands mention the possible formation of $PdNO_3^+$ and $Pd(NO_3)_2$, but also, for some of them, $Pd(NO_3)_3^-$ and $Pd(NO_3)_4^{2-}$. The values of the corresponding stability constants, β_i, proposed by these authors are consequently scattered (see Table 4). Note that in a very acidic medium, the existence of mixed hydroxy-nitrato Pd complexes, such as $PdOHNO_3$ pointed out by Camacho et al.,[9] can be excluded.

From each set of stability constants collected in Table 4, the distribution of the Pd(II) species formed in nitrate media is calculated and a mean NO_3^- ligand number is derived, which is plotted in Figure 7 as a function of the nitrate concentration. As expected, the resulting curves appear to depend strongly on the source used for the thermodynamic data. In Figure 7, the XAFS results of Table 3 are also reported. The mean ligand number calculated in the present work appears in good agreement with the values obtained by Jørgensen and Parthasarathy[2] as well as Camacho et al.[9] for low NO_3^- concentrations (less than 3 M) and confirms thus the weak complexation observed from spectrophotometric analysis. For high NO_3^- concentrations, a better agreement is observed with the values proposed by Tarapcik and derived from solvent extraction experiments.[10] The apparent disagreement observed between spectrophotometry and XAFS results for [NO_3^-] > 3 M can be due to the difficulty, for the former method, to deconvoluate accurately the optical spectra when more than three species are simultaneously present in the solution. In all the other works,[10−13] the Pd−nitrate complexation has been analyzed by extraction of palladium from nitric acid solutions. One of the authors, Shmidt et al.,[11] has pointed out that the proposed stability constants were calculated assuming that the activity coefficients remain practically constant in the considered nitric acid concentration range. The so-calculated β_i constants can only represent empirical parameters satisfying the expression for the Pd distribution coefficient between the two phases. Thus, these data should be also used with caution.

Conclusions

The hydration of Pd(II) ions in aqueous solutions was studied at room temperature by X-ray absorption spectroscopy. The XAFS above the Pd K-edge was interpreted using the MS approach. For the $Pd(H_2O)_4^{2+}$ square-planar aqua ion in strong perchloric acid, the use of an FEFF6 theoretical approach led to a first-shell Pd−O_w distance of 2.00 (1) Å with four water molecules and very small DW factor of $\sigma^2 = 0.0030$ (3) Å^2. The experimental XAFS FT signal can be well interpreted by taking into account the first coordination shell four planar water (2.0 Å) molecules and two or one axial water (2.5 Å) molecules with great DW factor, and by attributing the high-frequency component (3.7 Å) to the MS contribution originating within four planar water molecules.

This study has confirmed the formation of Pd−nitrate complexes in concentrated HNO_3 solutions. The radial distribution functions of these complexes are similar for the solid Pd-$(NO_3)_2(H_2O)_2$ with Pd−O and Pd−N distances of 2.0 and 2.8−2.9 Å, respectively. The first coordination shell XAFS spectra were fitted to calculate the mean NO_3^- ligand number around Pd(II). The results, obtained at a pH value close to zero, confirm those published both by Jørgensen et al.[2] and Camacho et al.[9]

Acknowledgment. We thank the "Laboratoire pour l'Utilization du Rayonnement ElectromagnÈtique" (LURE Orsay, France) for the beamtime allocation and laboratory facilities. We thank Dr. A. Maslennikov (Institute of Physical Chemistry, Russia) for his collaboration. J.P. expresses sincere thanks to Prof. I. Persson (Department of Chemistry, SLU Sweden), Dr. M. Benfatto (Laboratori Nazionali di Frascati − INFN, Italy), and Dr. L. Helm (Ecole Polytechnique Fèdèrale de Lausanne, Switzerland) for many helpful discussions.

Supporting Information Available: Three figures with FT and XANES information, and one table of fitting parameters.

This material is available free of charge via the Internet at http://pubs.acs.org.

References and Notes

(1) Elding, L. I. *Inorg. Chim. Acta* **1972**, *6*, 647.
(2) Jørgensen, C. K.; Parthasarathy, V. *Acta Chim. Scand.* **1978**, *A32*, 957.
(3) Helm, L.; Elding, L. I.; Merbach, A. E. *Helv. Chim. Acta* **1984**, *67*, 1453.
(4) Gröning, Ö.; Drakenberg, T.; Elding, L. I. *Inorg. Chem.* **1982**, *21*, 1820.
(5) Hellquist, B.; Bengtsson, L. A.; Holmberg, B.; Hedman, B.; Persson, I.; Elding, L. I. *Acta Chem. Scand.* **1991**, *45*, 449.
(6) Ayala, R.; Marcos, E. S.; Díaz-Moreno, S.; Solé, V. A.; Muñoz-Páez, A. J. Phys. Chem. B **2001**, *105*, 7588.
(7) Deeth, R. J.; Elding, L. I. *Inorg. Chem.* **1996**, *35*, 5019.
(8) Laligant, Y.; Ferey, G.; Le Bail, A. *Res. Bull.* **1991**, *26*, 269.
(9) Camacho, F. E.; Pitsch, H. K.; Ly, J.; Poitrenaud, C. *Talanta* **1995**, *42*, 1675.
(10) Tarapčik, P. *Radiochem. Radioanal. Lett.* **1981**, *49*, 353.
(11) Shmidt, V. S.; Mezkov, E. A.; Rubinsov, V. N.; Troyanovski, L. V.; Shorokhov, N. A. *Radiokhimiya* **1986**, *28*, 345.
(12) Zaitsev, B. N.; Inkova, E. N. *Radiokhimiya* **1981**, *23*, 817.
(13) El-Reefy, S. A.; Daoud, J. A.; Aly, H. F. *J. Radioanal. Nucl. Chem.* **1992**, *158*, 303.
(14) Vialard, E.; Germain, M. *Symposium on liquid−liquid extraction science*; Dounreay, U.K., 27−29 Nov. 1984.
(15) Martínez, J. M.; Torrico, F.; Pappalardo, R. R.; Marcos, E. S. *J. Phys. Chem. B* **2004**, *108*, 15851.
(16) Johansson, L. *Coord. Chem. Rev.* **1974**, *12*, 241.
(17) Pearson, R. G. *J. Am. Chem. Soc.* **1963**, *85*, 3533.
(18) Van Middlesworth, J. M.; Wood, S. A. *Geochem. Cosmochem. Acta* **1999**, *63*, 1751.
(19) Richens, D. T. *The Chemistry of Aqua Ions*; John Wiley & Sons: New York, 1997.
(20) Kuzmin, A. *Physica B* **1995**, *208−209*, 175.
(21) Moreau, G.; Helm, L.; Purans, J.; Merbach, A. E. *J. Phys. Chem. A* **2002**, *106*, 3034.
(22) Chaboy, J.; Tyson, T. A.; *Phys. Rev. B* **1994**, *49*, 5869.
(23) Rehr, J. J.; Mustre de Leon, J.; Zabinsky, S. I.; Albers, R. C. *J. Am. Chem. Soc.* **1991**, *113*, 5135.
(24) Caminiti, R.; Sadun, C.; Basanisi, M.; Carbone, M. *J. Mol. Liq.* **1996**, *70*, 55.
(25) Caminiti, R.; Carbone, M.; Sadun, C. *J. Mol. Liq.* **1998**, *75*, 149.
(26) Frenkel, A. I.; Korshin, G. V.; Ankudinov A. L., *Environ. Sci. Technol.* **2000**, *34*, 2138.
(27) Campbell, L.; Rehr, J. J.; Schenter, G. K.; McCarthy, M. I.; Dixon, D. *J. Synchrotron Radiat.* **1999**, *6*, 310.
(28) Benfatto, M.; D'Angelo, P.; Della Longa, S.; Pavel, N. V. *Phys. Rev. B* **2002**, *65*, 174205.
(29) Muñoz-Páez, A.; Pappalardo, R. R.; Marcos, E. S. *J. Am. Chem. Soc.* **1995**, *117*, 11710.
(30) Sakane, H.; Muñoz-Páez, A.; Díaz-Moreno, S.; Martínez, J. M.; Pappalardo, R. R.; Marcos, E. S. J. Am. Chem. Soc. **1998**, *120*, 10397.
(31) Kuzmin, A.; Obst, S.; Purans, J. *J. Phys*: *Condens. Matter* **1997**, *9*, 10065.